

# Experimental and Analytical Study of Grouted Sleeve Splice Under Axial Tensile Load



Abdallh M. Soliman, Hatem H. Ibrahim, Hossam A. Hodhod

**Abstract:** Paper Compared to traditional cast-in-place concrete structures, the precast Concrete structures are usually constructed in a controlled environment, i.e. plants, and then assembled through certain links at the construction site. The concrete precast concrete structures can therefore have better concrete quality and help to reduce labor costs and increase construction speed. Because of these advantages, in recent years the precast concrete structures have received much attention. This research work therefore presents a reasonable procedure for designing a grouted sleeve splice connection using a simple material such as standard pipes with little workmanship which gives the design a good advantage compared to just using selection tables for expensive proprietary similar connection. Such splices' mechanical behavior is a function of two essential mechanisms: bar-to-grout bond behavior, and sleeve-to-grout bond behavior. To achieve the purpose of this analysis work, three arrangements were manufactured and checked under incremental axial tensile load with an all-out number of 66 grouted sleeve specimens. While experimental methods of investigation are extremely useful in obtaining information about the grouted sleeve connection behavior, the use of numerical models helps to develop good comprehension of behavior at lower cost. Models of non-linear finite-element analysis for grouted sleeve connection were presented in this research. The research utilized the commercial Finite Element modeling software (ANSYS) to study the effects of some parameters that are important in the bond behavior of the grouted sleeve connection and compare the analytical results with the experimental results to confirm the analytical model. The average efficiency of the finite element models using ANSYS was 92.5%. Having the finite element model validated, a parametric study was performed using ANSYS to evaluate the effect of the following parameters on the behavior of grouted sleeve: bar diameter, embedded length, grout compressive strength, sleeve wall thickness, and sleeve inner diameter.

**Keywords :** Precast concrete; connection; Grouted; splice; Mechanical Splice; Confinement; Bond Behavior; Finite Element; bar embedment length; Material nonlinearity.

## I. INTRODUCTION

Precast concrete buildings have gained popularity around the world, see Fig. 1.

Buildings which were already constructed with cast-in-situ concrete can be constructed with precast concrete components prefabricated within the factories.

These ready-made loose components such as precast concrete wall panels are introduced on site. Too, the association can extend the structural integrity of precast concrete components. A grouted splice could be a type of mechanical connectors that utilized as the connections for precast concrete structures. Figure 2 appears a few common applications of mechanical splices in precast concrete structures, where they can be utilized as the column-to-base, wall – to – wall, column – to – column, beam-to-beam connections. Splice connectors are cast along with precast components some time recently transported to the construction sites.

In order to assemble the precast elements, the steel bars projecting from them are inserted and grouted within the connectors embedded within the other components. The preferences of splice connectors include ease of installations that speed up the construction pace, way better bond efficiency under proper confinement that leads to shorter required bar development length and others.



Fig. 1 : Precast Concrete Building

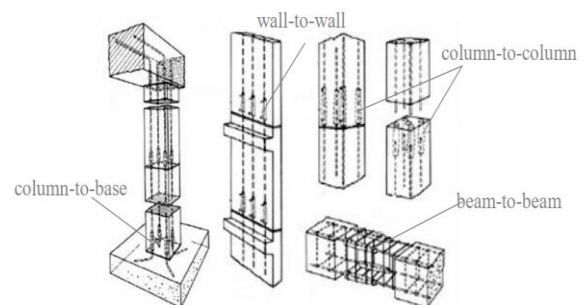


Fig.2 : Application of mechanical Splice.

Revised Manuscript Received on November 30, 2020.

\* Correspondence Author

Abdallh M. Soliman \*, lecturer Assistant, October High Institute, OHI, Giza, Egypt. Email: eng.abdallhmostafa@yahoo.com

Hatem H. Ibrahim, Assistant Professor, Cairo University, Giza, Egypt. Email: [Hibrahim@kdassociates.com](mailto:Hibrahim@kdassociates.com)

Hossam A. Hodhod, professor, Cairo University, Giza, Egypt. Email: [hodhodh2002@yahoo.com](mailto:hodhodh2002@yahoo.com)

© The Authors. Published by Blue Eyes Intelligence Engineering and Sciences Publication (BEIESP). This is an open access article under the CC BY-NC-ND license (<http://creativecommons.org/licenses/by-nc-nd/4.0/>)

## II. PREVIOUS WORK

This Researchers The structural performance and durability of reinforced concrete individuals are exceedingly subordinate on the bond strength between strengthening steel bars and the encompassing concrete. Bond strength may be a work of the confinement given by the concrete itself and transverse reinforcement that encompasses reinforcing steel bars.

Transverse confinement plays a basic part in deciding the specified improvement length and/or splice length. The taking after segment shows up a study of the explore work accessible inside the composing, examining the mechanical behavior of the sleeves beneath tensile load. Bond between steel and concrete is basic for the judgment of any strengthened concrete structure. Nevertheless, bond could be a complex issue and depends on numerous parameters. Due to its significance for practical design, the think about of bond between steel and concrete has continuously been a popular issue in the field of research.

According to Untrauer and Henry [15], bond can be defined as the adhesion of mortar to reinforcement bar or to other surfaces against which it is set. Bond strength between the steel and concrete increases in degree to square root of ordinary pressure and mortar strength. Normal pressure was connected to the faces of concrete specimens subjected to tensile forces. Lutz [10], and M.K[11]. Thompson [14] talk about the principles of bond, where the bond between steel bar and mortar is contributed by three major variables, to be particular chemical adhesion, friction, and mechanical interlocking between bar ribs and mortar keys, of which for the foremost portion concurred that the mechanical interlocking mechanism is for the most part more critical. Soroushian [13], who explored the local bond stress behavior of deformed bars in confined mortar, concluded that the bond strength diminished linearly as the bar diameter increased. In order to assess the performance of mechanical connectors, the specimens are commonly tested experimentally beneath incremental tensile loads, such as already conducted by Einea [8], Coogler [5], and Jansson [9]. A satisfactory splice is recognized based on their failure modes, where the spliced steel bars ought to fracture outside of the sleeve, indicating palatable bond strength that outperforms the tensile strength of steel bars.

Einea et al. [8] surveyed the bond strength of strengthening bars as a work of grout compressive strength and the level of confinement by considering the variables that impact the bond strength of reinforcing bars limited with steel channels. They point by point that a advancement length as short as seven time the bar diameter can be fulfilled by confining the high quality grout encompassing the bars. In terms of ultimate tensile performance, relevant codes, such as ACI. 318 [2] and ECP [7], indicate that an satisfactory mechanical splice should be able to offer the connection strength at least 25 percent higher than the specific yield strength of the spliced bars. Dar win et al. [3] concluded that the fourth root of the concrete strength given an exact representation of the effect of concrete strength on bond strength, and the yield strength of transverse reinforcement plays no basic part in choosing the improvement length.

Einea et al. [8] inspected the behavior of spirally confined lap splices of deformed reinforcing bars in concrete. They concluded that joins with two lapping bars joined to the main bars appeared the most excellent performance. Moreover, they detailed that the ACI [2] condition overestimates the desired lap length by at slightest 76%. They suggested to postpone the 12 in. constrain on least length of a lap join and increment the constrain on the confinement term to 4 instead of 2.5.

AbdAllh [1] study divers sleeve size and configuration and derived equations that could be used to determine the embedded length taking into consideration the grout compressive strength, bar diameter, confining strength, sleeve inner diameter and the sleeve wall thickness. Equation 1, 2 and 3.

$$tbi = 0.75\sqrt{fg} \quad (1)$$

$$\frac{Ub}{\sqrt{fg}} = 0.0064 * ds_{in} + 0.1871 * ts + 0.0648 * db - 0.006 * Lb \quad (2)$$

$$\frac{Ub}{\sqrt{fg}} = 1.747 - 2.45 * 10^{-3} * ds_{in} + 0.05976 * ts + 8.475 * 10^{-2} * db - 8.84 * 10^{-3} * Lb \quad (3)$$

Where:

$fg$  = grout compressive strength (MPa)

$tbi$  = initial bond strength (MPa)

$Ub$  = bond strength of bar - to - grout (MPa)

$ds_{in}$  = inner diameter of (mm)

$ts$  = sleeve wall thick ness (mm)

$db$  = spliced bar diameter (mm)

$Lb$  = spliced bar embedded length (mm)

Belal [4] derived equation to evaluate the minimum numbers of grooves which can prevent the grout to sleeve bond failure equation 4, 5 and 6.

Where:

$P_t$  = Total force resisted by the grouted splices (N)

$P_s$  = Force resisted by the grout-sleeve bond action (N)

$P_{gr}$  = Force resisted by the grooves (N)

$\mu_s$  = Coefficient of friction between the sleeve and grout = 0.05

$ld$  = bar embedded length (mm)

$h_{gr}$  = Height of the grooves (mm)

$n_{gr}$  = Number of grooves per embedded length

$\mu_g$  = Shear friction coefficient of the grout (monolithically cast) = 1.4

$fn$  = Confinement stress as per Eqn. (4.4) (N/mm<sup>2</sup>)

$$P_t = P_s + P_{gr} \quad (4)$$

$$P_s = f_n \pi d_{si} (ld - h_{gr} n_{gr}) \quad (5)$$

$$P_{gr} = (\mu_g f_n + v_g) d_{si} h_{gr} n_{gr} \quad (6)$$

$v_g$  = shear strength of the grout (N/mm<sup>2</sup>).

### III. OBJECTIVES

The objective of this research work was to create the Computational model of the grouted splice sleeve connectors. And compare the results with the lab results of AbdAllh [1] to confirm the results. After verifying the model, a parametric study was performed using ANSYS to evaluate the effect of the following parameters on the behavior of grouted splice sleeve: bar diameter, embedded length, grout compressive strength, sleeve wall thickness, and sleeve inner diameter.

### IV. FINITE ELEMENT MODELING

#### A. Description of Specimens:

Two types of models were developed, the first model for Grouted spliced Sleeve (GSS) specimens as shown in Figure 3 and the second model for the Grouted Spliced Sleeve with Ring (GSSR) specimens as shown in Figure 4.

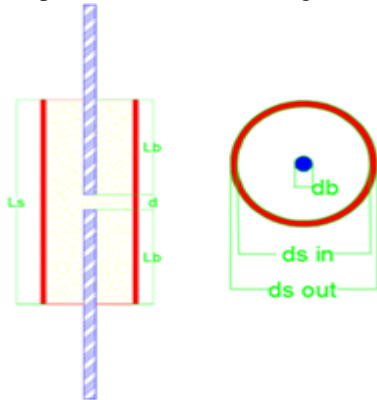


Fig. 3 Details of GSS Specimens

#### B. Modeling assumptions:

The following are the modeling assumptions made for the grouted splice sleeve connection models in the present study to provide reasonably good simulations for the complex behavior:

- Concrete and steel are modeled as isotropic and homogeneous materials.
- Poisson's ratio is assumed to be constant throughout the loading history.
- Steel is assumed to be an elastic-perfectly plastic material and identical in tension and compression.
- Perfect bond exists between grout and steel reinforcement.
- Time-dependent nonlinearities such as creep, shrinkage, and temperature change are not included in this study

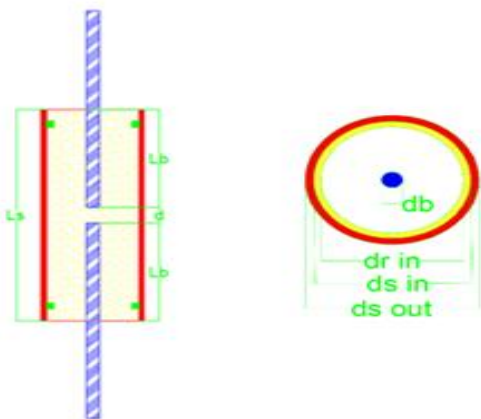


Fig. 4 Details of GSSR Specimens

### C. Stage of finite element model

There are five main stages to model any specimen:

- Defining element types, real constants, and material properties.
- Modeling the geometry of grouted splice sleeve connection specimens.
- Meshing the specimen geometry.
- Applying boundary conditions and loads on specimen.
- Loading procedure and analysis of the results.

#### 1) Define element types and material properties

In this section, the description of element types used for all materials used in ANSYS models is presented. These materials are grout, steel reinforcement, sleeve, and ring as illustrated in Table 1. Elements used in thesis models are widely used and recommended by ANSYS.

Table 1: Element types in ANSYS for FEM

Material type	ANSYS element type
Grout	Solid65
Reinforcement	Link180
Sleeve and Ring	Solid185

#### 2) Define element types

##### a) Grout

SOLID65 is used for the 3-D modeling of solids with or without reinforcing bars (rebar). The solid is capable of cracking in tension and crushing in compression. In concrete applications, for example, the solid capability of the element may be used to model the concrete while the rebar capability is available for modeling reinforcement behavior. The element is defined by eight nodes having three degrees of freedom at each node: translations in the nodal x, y, and z directions as shown in Figure 5. The concrete element is like a 3-D structural solid but with the addition of special cracking and crushing capabilities. The most important aspect of this element is the treatment of nonlinear material properties. The concrete is capable of cracking (in three orthogonal directions), crushing, plastic deformation, and creep. The rebar is capable of tension and compression, but not shear. (ANSYS Mechanical APDL Manual Set, (2012) [16])

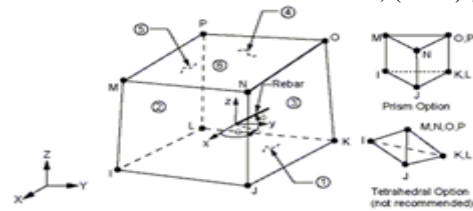


Figure 5: Solid65 geometry (ANSYS Mechanical APDL Manual Set, (2012) [16]).

##### b) Reinforcement

LINK180 is a 3-D spar that is useful in a variety of engineering applications. The element can be used to model trusses, sagging cables, links, springs, and so on. The element is a uniaxial tension-compression element with three degrees of freedom at each node: translations in the nodal x, y, and z directions as shown in Figure 6.



## Experimental and Analytical Study of Grouted Sleeve Splice Under Axial Tensile Load

Tension-only (cable) and compression-only (gap) options are supported. As in a pin-jointed structure, no bending of the element is considered. Plasticity, creep, rotation, large deflection, and large strain capabilities are included.

By default, LINK180 includes stress-stiffness terms in any analysis that includes large-deflection effects. Elasticity, isotropic hardening plasticity, kinematic hardening plasticity, Hill anisotropic plasticity, Chaboche nonlinear hardening plasticity, and creep are supported. To simulate the tension-/compression-only options, a nonlinear iterative solution approach is necessary; therefore, large-deflection effects must be activated (NLGEOM,ON) prior to the solution phase of the analysis. Added mass, hydrodynamic added mass and loading, and buoyant loading are available. (ANSYS Mechanical APDL Manual Set, (2012) [16]).

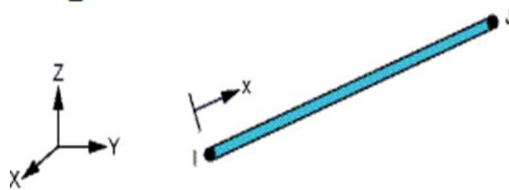


**Figure 6: Link180 geometry (ANSYS Mechanical APDL Manual Set, (2012) [16]).**

### c) Sleeve and ring

SOLID185 Structural Solid is suitable for modeling general 3-D solid structures. It allows for prism, tetrahedral, and pyramid degenerations when used in irregular regions. Various element technologies such as B-bar, uniformly reduced integration, and enhanced strains are supported. The geometry and node locations for this element are shown in Figure 7: SOLID185 Homogeneous Structural Solid Geometry. The element is defined by eight nodes and the orthotropic material properties. The default element coordinate system is along global directions. (ANSYS Mechanical APDL Manual Set, (2012) [16]).

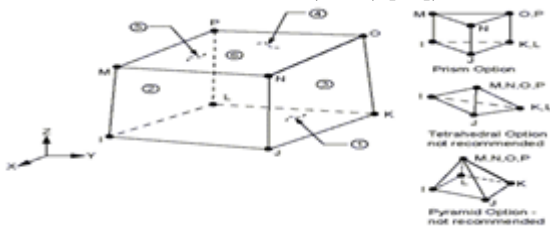


**Figure 7: Solid185 geometry (ANSYS Mechanical APDL Manual Set, (2012) [16]).**

### 3) Define material properties

#### a) Model of grout

Material Model Number 1 refers to the Solid65 element. The Solid65 element requires linear isotropic and multilinear isotropic material properties, in addition to selection of failure criteria of concrete.

- Linear isotropic properties for grout material

EX is the modulus of elasticity of the grout ( $E_c$ ). It was based on the sika grout data sheet [12] and its equal to 37000MPa. PRXY is the Poisson's ratio ( $\nu$ ). Poisson's ratio was assumed to be 0.2

- Multi linear isotropic properties for grout material

The actual compressive strength for grout  $F_g$  and the corresponding strain used to define the multi linear behavior.

Also, the program can draw the stress strain curve for grout as shown in Figure 8.

- Failure criteria for grout

Open shear transfer coefficient = 0.20

Closed shear transfer coefficient = 0.80

Uniaxial cracking stress  $f_{ctr} = 0.60\sqrt{f_g}$  (7)

Uniaxial crushing stress  $f_c = -1$

Biaxial crushing stress = 0.00

Hydrostatic pressure = 0.00

Hydrostatic biaxial crush stress = 0.00

Hydrostatic uniaxial crush stress = 0.00

Tensile crack factor = 0.00

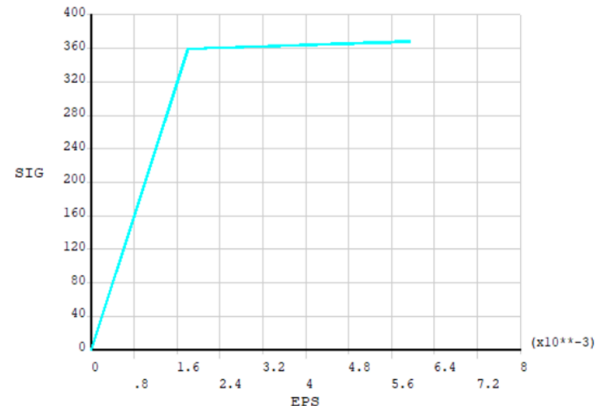


**Figure 8: Stress strain curve for grout material.**

#### b) Model of reinforcement

Material Model Number 2 refers to the link185 element. The link185 element

requires linear isotropic and multilinear isotropic material properties.

- Linear isotropic properties for reinforcement material

EX is the modulus of elasticity of the reinforcement ( $E_s$ ) and its assumed to be 200000 MPa. PRXY is the Poisson's ratio ( $\nu$ ). Poisson's ratio was assumed to be 0.3

- Bilinear isotropic properties for reinforcement material

The bilinear model requires the Yield Stress ( $f_y$ ) which assumed to be 360 MPa, as well as the Hardening Modulus (tangent modulus of the plastic region) of steel which assumed to be 2000 MPa. Also, the program can draw the stress strain curve for reinforcement as shown in Figure 9.

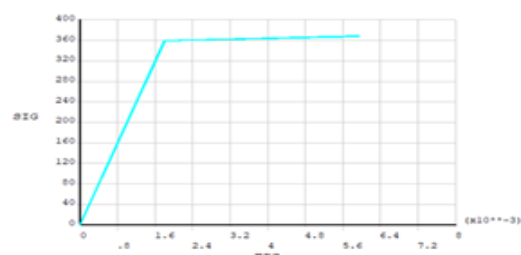


**Figure 9: Stress strain curve for reinforcement material.**

#### c) Model of sleeve

Material Model Number 3 refers to the solid185 element. The link185 element requires linear isotropic and multilinear isotropic material properties.

- Linear isotropic properties for reinforcement material  
EX is the modulus of elasticity of the reinforcement ( $E_s$ ) and its assumed to be 200000 MPa. PRXY is the Poisson's ratio ( $\nu$ ). Poisson's ratio was assumed to be 0.3.

- Bilinear isotropic properties for reinforcement material  
The bilinear model requires the Yield Stress ( $f_y$ ) which assumed to be 240 MPa, as well as the Hardening Modulus (tangent modulus of the plastic region) of steel which assumed to be 0 MPa. Also, the program can draw the stress strain curve for sleeve as shown in Figure 10.

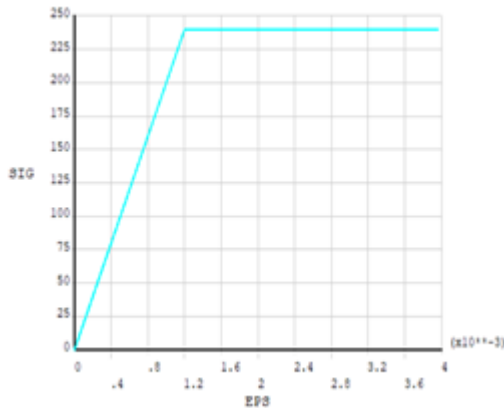


Figure 10: Stress strain curve for Sleeve material.

#### 4) Geometry of grouted splice sleeve connection

This model consists of four parts, the first part is sleeve was modeled as volume as shown in Figure 11 and the second part is grout was modeled as volume as shown in Figure 12. In addition, the third and the fourth parts were the embedded reinforcement bar. The reinforcement bars were modeled as lines as seen in Figure 13.

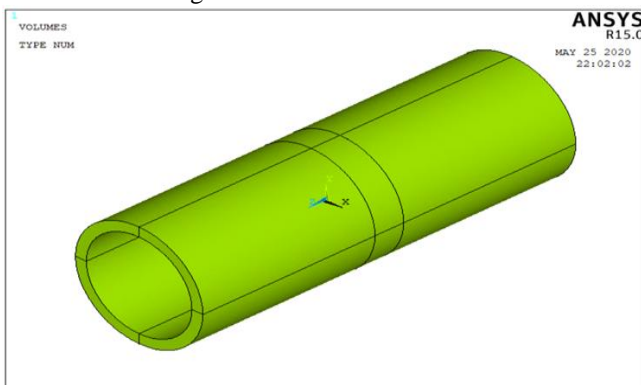


Figure 11: Sleeve Model.

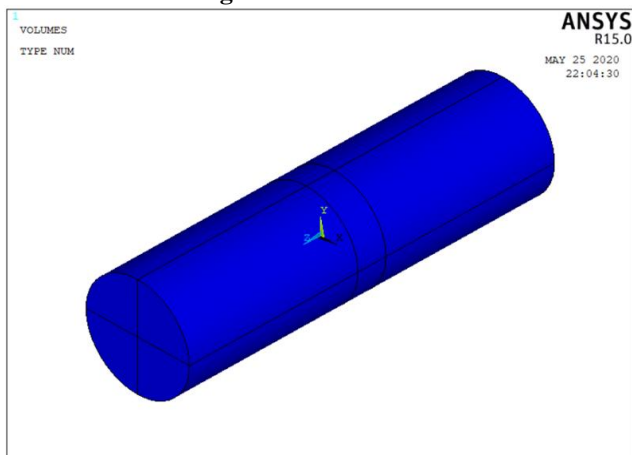


Figure 12: Grout Model.

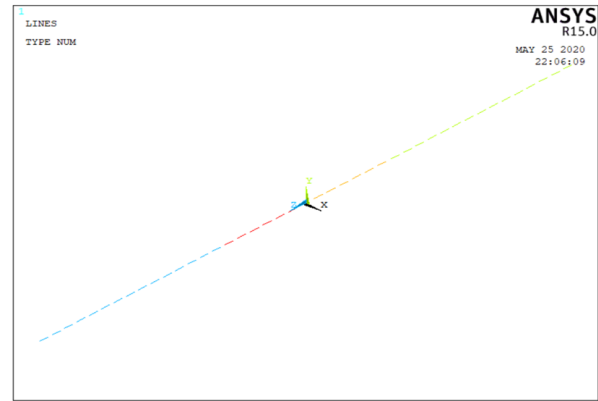


Figure 13: Reinforcement Bar Model .

#### 5) Meshing the Specimen Geometry

To obtain good results from the Solid65 element, the use of a rectangular mesh is recommended. Therefore, the mesh is set up such that square or rectangular elements are created. Reinforcement bars and sleeve were meshed as solid elements in such a way that its nodes were oriented with adjacent grout solid elements. The overall mesh of the concrete beam and steel plates' volumes for flexure beam model is shown in Figure 14.

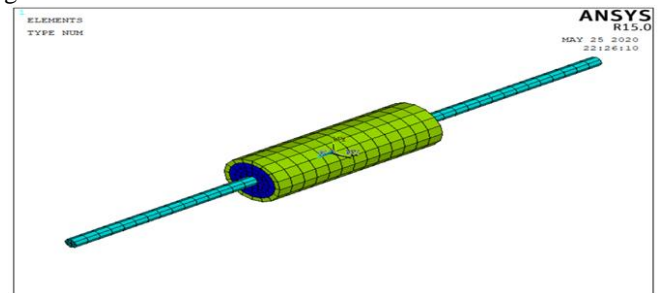


Figure 14: Meshing of grouted spliced sleeve model.

#### 6) Boundary conditions, supports and applied loads

Displacement boundary conditions are needed to constrain the model to get a unique solution. To ensure that the model acts the same way as the experimental specimen; boundary conditions need to be applied at points of symmetry, and where the supports and loadings exist. The applied load is assumed as Z direction displacement at the end of the first bar and the end of the second bar was assumed to be fixed in all directions as shown in Figure 15.

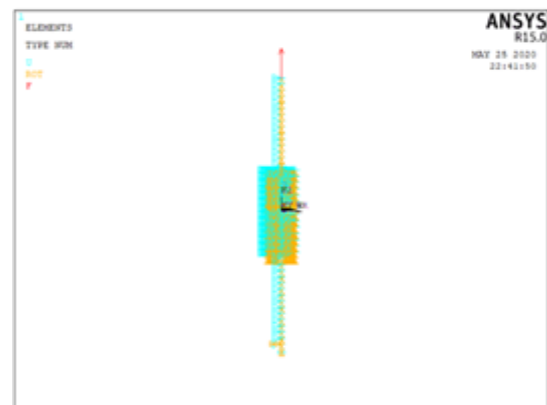


Figure 15 : load and supports of mode.

## 7) Setting nonlinear solution parameters

Setting solution parameters involves defining the analysis type and common analysis options for an analysis, as well as specifying load step options for it. To ignore large deformation effects such as large deflection, large rotation, and large strain; the analysis option was set to (Small Displacement Static).

In nonlinear analysis, the load applied to the structures must be increased gradually to avoid non-convergence. The total load applied to a finite element model is divided into a series of load increments called load steps. At the completion of each incremental solution, the stiffness changes in structural stiffness before proceeding to the next load increment.

The ANSYS program uses Newton–Raphson equilibrium iterations for updating the model stiffness. Automatic time stepping in the ANSYS program predicts and controls load step sizes. Based on the previous solution history and the physics of the models, if the convergence behavior is smooth, automatic time stepping will increase the load increment up to a selected maximum load step size. If the convergence behavior is abrupt, automatic time stepping will bisect the load increment until it is equal to a selected minimum load step size. The maximum and minimum load step sizes are required for the automatic time stepping.

Nonlinear Static Analysis type was utilized for grouted splice sleeve.

## V. VERIFICATION OF ANSYS FINITE ELEMENT MODELS

Tensile force of the modeled specimens was obtained from the program as shown in Figure 16 where the time refers to the tensile force as mentioned before for example time = 1000 that is means the tensile force equal 1 kN.

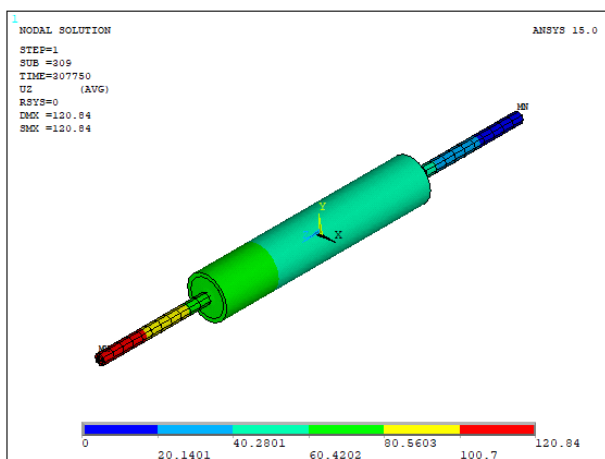


**Figure 16: Tensile force obtained from ANSYS model.**

We can also get the bar stress, grout stress, and the Sleeve stress from the program as shown in figures 17, 18, and 19 respectively.

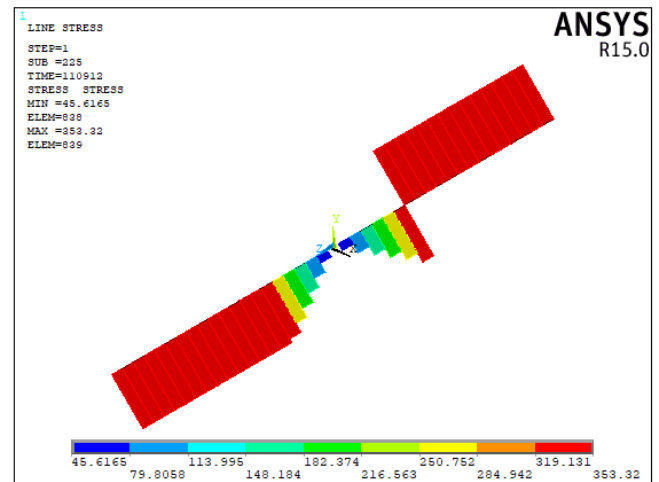


**Figure 17: Bar stress.**

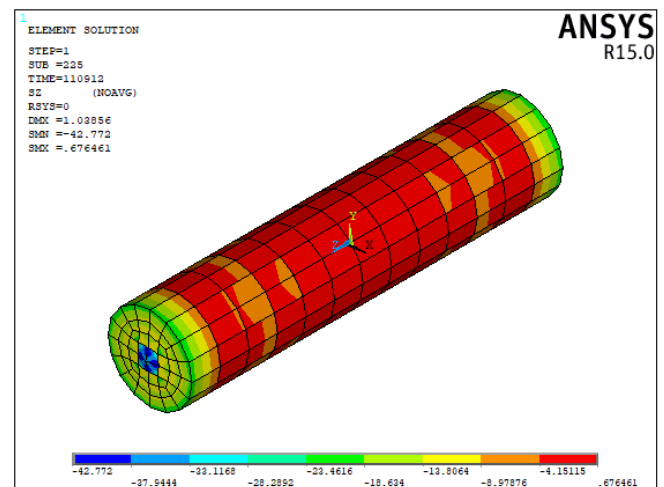


**Figure 18: Grout stress.**

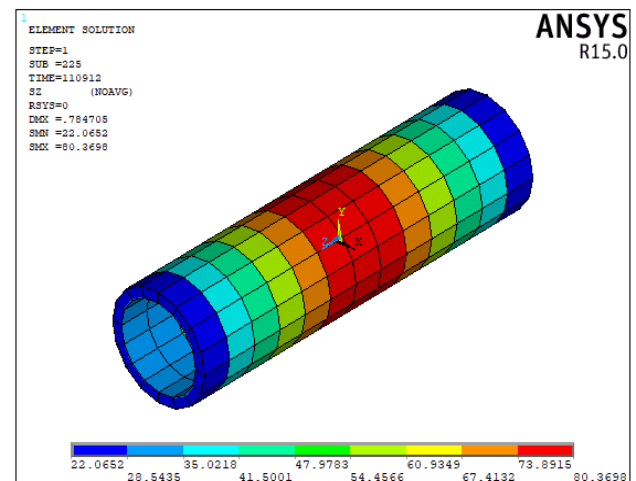


**Figure 19: Sleeve stress.**

We can note the bar fracture failure when the bar stress exceeds the ultimate strength of bar which defined before with value 520 MPa as shown in Figure 20.

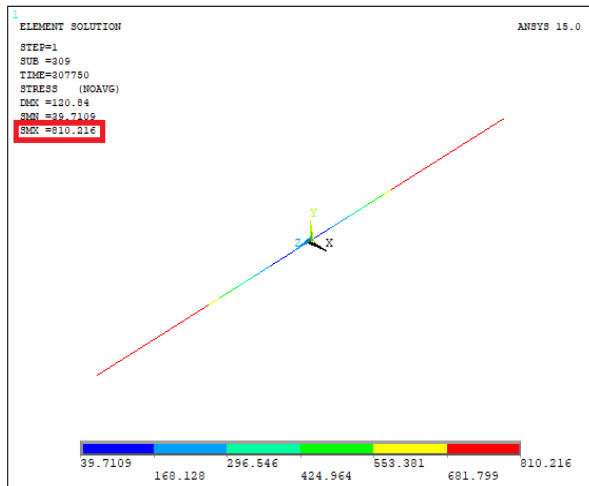


Figure 20: Bar fracture failure .

The bar to grout failure occurs when the rebar stress doesn't reach the ultimate strength, but the grout stress doesn't exceed the grout compressive strength as shown in figure 21.

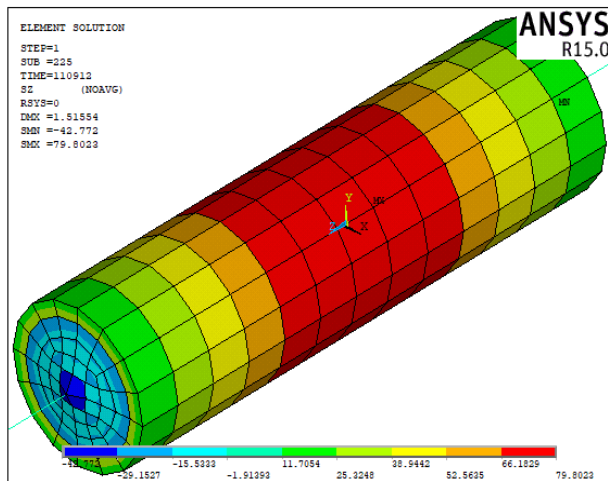


Figure 21: bar to grout Failure.

The grout to sleeve failure failure occurs when the rebar stress doesn't reach the ultimate strength, but the grout stress exceeds the grout crushing strength as shown in figure 22.

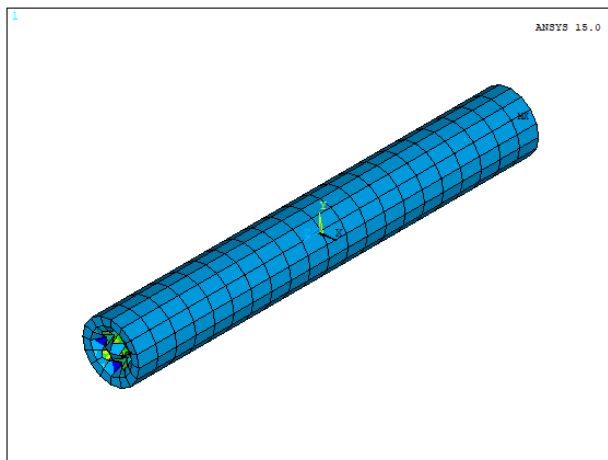


Figure 5. 31: Grout to sleeve Failure.

The finite element models developed for GSS and GSSR specimens were verified by comparing results obtained from the FE analysis with results obtained from corresponding experimental tests for 20 specimens. The verification process was based on the following criteria: Tensile load , and Failure

mode. In addition, the model efficiency percentage  $\eta$  were calculated by dividing the tensile force obtained from Ansys model by the tensile force obtained from the tested specimens. The model efficiency percentage  $\eta$  ranged from 81.6% to 99.2% and the average model efficiency percentage is equal to 92.6% which mean good agreement between the Ansys model and the tested specimens. Table AP 1 shows the comparison between the test results and analytical model results. The difference between the tested results and the analytical results may be attributed to the fact the program stops the analysis process when any one of the materials reaches the defined material max stress but in the lab the testing process continues.

## VI. PARAMETRIC STUDY

Having the finite element model validated, a parametric study was performed using ANSYS to evaluate the effect of the following parameters on the behavior of grouted splice sleeve: bar diameter , embedded length, grout compressive strength, sleeve wall thickness, and sleeve inner diameter.

The used bar diameters were 12mm, 16mm, 20mm, and 22mm. Three types of grout were used G200, G214, and G295 with compressive strength equals to 50MPa, 70MPa, and 80MPa respectively. Four different sleeves were used namely: SL48, SL60, SL73, and SL88. Three different embedded length were used 6 $\phi$ , 8 $\phi$ , and 10 $\phi$ . Table 2 shows the studied parameters.

36 specimens were modeled using the verified ANSYS model. Table AP 2 shows the modeled specimens results summary including the tensile force and the mode of failure of the modeled specimens.

Table 3: The studied parameters.

Grout Type	G200	G214	G295	
Grout compressive strength (Fg)	50 MPa	70 Mpa	80 MPa	
Bar diameter ( $\phi$ )	12 mm	16 mm	20 mm	22 mm
Bar embedded length	6 $\phi$	8 $\phi$	10 $\phi$	
Sleeve name	SL48	SL60	SL73	SL88
Sleeve outside diameter (d out)	48.26	60.33	73.03	88.9
Sleeve inside diameter (d in)	33.98	42.85	59.01	73.66
Sleeve wall thickness (ts)	7.14	8.74	7.01	7.62

## VII. FEM SUMMARY AND CONCLUSIONS FROM THE PARAMETRIC STUDY THE FOLLOWING BECOMES CLEAR

- o the tensile stress increased by increasing of bar size.
- o the tensile stress increased by increasing of embedded length.
- o the tensile stress increased by increasing of grout compressive strength .
- o Increasing compressive strength of the grout increase the strength of the initial bond and the total force of the bond.



- o with the increase of embedded length, bar diameter, and wall thickness the total bond strength increases.
- o Increasing the diameter of the inside sleeve reduces the total strength of the bond.
- o the model efficiency percentage  $\eta$  ranged from 89.42% to 105.22% and the average model efficiency percentage is equal to 99.88% which mean good agreement between the Ansys model and the tested specimens. Table AP 3 shows the comparison between the parametric study results and derived equation 2 results.

## VIII. CONCLUSIONS

- Increasing compressive strength of the grout increase the strength of the initial bond and the total force of the bond.
- With the increase of embedded length, bar diameter, and wall thickness the total bond strength increases.
- Increasing the diameter of the inside sleeve reduces the total strength of the bond.
- The addition of interlocking steel rings at both ends of the interior sleeve wall greatly improved the grouted bar splice 's tensile capacity. constraining the grout within the sleeve prevents the grout-sleeve bond and enhances the confining stress which also increases the bar-grout bond strength.
- The introduction to both ends of the inner sleeve wall of interlocking steel rings with a minimum thickness of 7 mm was adequate and the tensile strength of the spliced bars was achieved. The steel rings prevent the grout the grout to sleeve bond failure.
- Finite element model using ANSYS was successfully verified comparing with experimental test results. Therefore, ANSYS can be confidently used in analysis of grouted splice sleeve connection.
- The average efficiency of the finite element models using ANSYS was 92.5%.

## REFERENCES

1. AbdAllh Mostafa "The Mechanical behavior of grouted sleeve splice connections with and without mechanical interlocking ring under axial tensile load"2020.
2. ACI 318 -14 (2014), Building Code Requirements for Structural Concrete and Commentary, Building Code Requirements for Structural Concrete (ACI 318-14) An ACI Standard Commentary on Building Code Requirements for Structural Concrete (ACI 318 R-14) An ACI Report, American Concrete Institute; Michigan, United States.
3. ASTM A106 Grade B, ASTM A106 / A106M - 15 Standard Specification for Seamless Carbon Steel Pipe for High-Temperature Service; ASTM INTERNATIONAL. (2015) <https://www.astm.org/Standards/A106.htm>
4. Belal Ali "Experimental study of the mechanical behavior of grouted spliced sleeve connections for precast concrete construction under axial load" 2016.
5. Coogler KL, Harries KA, Gall ick M. Experimental study of offset mechanical lap splice behavior. A.C.I. Struct J 2008 ; 105 (4) : 478 – 87
6. Darwin, ZuoJ, TholenML, Idun EK. Development length criteria for conventional and high relative rib area reinforcing bars. ACI Struct J 1996 ;93 (3) : 1–13.
7. ECP (2018), Egyptian Code of Practice: ECP 203 - 2007, Egyptian Code for Design and Construction of Concrete Structures (ECP 203 - 2018 ), Housing and Building National Research Center; Giza, Egypt.
8. Einea, and Tadros, M.K. (1995), "Grout-Filled Pipe Splices for Precast Concrete Const ruction", P. C. I Journal , 40 (1) , 82–93.

9. Jansson PO. Evaluation of grout-filled mechanical splices for precast concrete, Construction. T. I. -2094; 2008
10. Lutz, L. A., and Gergely, P., Mechanics of Bond and Slip of De formed Bars in Concrete, ACI. Journal, American Concrete Institute, Vol. 64 , No . 11 , 1967
11. Mahdi, M., Ah. mad, J., and Ar. ash, K. 2003, Bond of cement grouted rein forcing bars under constant radial pressure, Master Project, University Technology Malaysia, 2003
12. S I K A grout @ 200 (2015), Sika grout® -200 High strength, Non-shrink, None oxidized Cementitious Grout; Sika Egypt for Construction Chemicals, El About City, Egypt.
13. Soroushian P, Ch. oi KB, Park GH, Asl. ani F. Bond of deformed bars to concrete effects of confinement and strength of concrete. A. C. I. Mater J 1991 ; 88 (3) : 227 – 32.
14. Thompson JN. Lap ped splices in rein forced concrete beams. Proc J Am Concrete Inst 1955 ; 52 (2) : 201 – 12.
15. Untrauer RE, Henry RL. Influence of normal pressure on bond strength. A. C. I. J 1965 ; 62(5) :5
16. Manual, A. U. S. (2015). ANSYS Mechanical APDL Technology Demonstration Guide. Canonsburg, ANSYS Inc, USA.

## AUTHORS PROFILE



**Abdallah M. Soliman** - PhD student at structural department faculty of engineering Cairo university. He has master's in science in concrete to his credit. His area of research is precast concrete specially the splice between concrete and steel reinforcement. He has published paper in the field of concrete - concrete composite section



**Hatem H. Ibrahim**- he is an assistant professor in department of structural at faculty of engineering Cairo university. He has master's in science from Cairo university and PhD degree from university of Alberta Canada .



**Hossma A. Hodhod** - he is a professor in department structural at faculty of engineering Cairo university. He has master's in science from Cairo university and PhD degree from university of Tokyo. He has published many papers in the field of properties and strength of materials.



## Appendix

**Table AP 1: The results of the Ansys models verses the results tested specimens .**

ID	Sleeve				Bar		Grout	F (Tested)	F (Ansys)	$\eta$ %	Mode of Failure From Lab
	ds out	ts	ds in	Ls	$\phi$	Lb	Fg				
	mm	mm	mm	mm	mm	mm	Mpa	Kn	Kn		
GSS 1	88.9	7.62	73.66	260	18	120	68	136	128.6	94.6	grout to sleeve bond failure
GSS 3	88.9	7.62	73.66	420	18	200	68	151	139.1	92.1	bar fracture
GSS 4	88.9	5.49	77.92	260	18	120	62	116.6	114.2	97.9	grout to sleeve bond failure
GSS 5	88.9	5.49	77.92	340	18	160	62	126.7	119.6	94.4	grout to sleeve bond failure
GSS 6	88.9	5.49	77.92	420	18	200	62	131	126.4	96.5	grout to sleeve bond failure
GSS 7	88.9	7.62	73.66	260	18	120	75	140	137.5	98.2	grout to sleeve bond failure
GSS 8	88.9	7.62	73.66	340	18	160	75	148.2	143.6	96.9	grout to sleeve bond failure
GSS 9	88.9	7.62	73.66	420	18	200	75	151.7	148.6	98.0	bar fracture
GSS 10	73.03	7.01	59.01	260	18	120	75	146.7	128.7	87.7	grout to sleeve bond failure
GSS 11	73.03	7.01	59.01	340	18	160	75	151.7	132.7	87.5	grout to sleeve bond failure
GSS 12	73.03	7.01	59.01	420	18	200	75	154	148.7	96.6	bar fracture
GSS 16	101.6	5.74	90.12	270	25	125	67	204	172.7	84.7	bar grout bond failure
GSS 17	101.6	5.74	90.12	320	25	150	67	238	197.5	83.0	bar grout bond failure
GSS 18	101.6	5.74	90.12	420	25	200	67	295	287	97.3	bar grout bond failure
GSS 24	114.3	8.56	97.18	420	32	200	68	457.5	420	91.8	bar fracture
GSSR 1	88.9	7.62	73.66	260	18	120	68	138.2	128.5	93.0	bar grout bond failure
GSSR 2	88.9	7.62	73.66	340	18	160	68	147.5	133.3	90.4	bar fracture
GSSR 3	88.9	7.62	73.66	420	18	200	68	152.5	137.5	90.2	bar fracture
GSSR 4	88.9	5.49	77.92	260	18	120	68	116.2	115.3	99.2	bar grout bond failure
GSSR 5	88.9	5.49	77.92	340	18	160	68	149.8	122.2	81.6	bar grout bond failure

# Experimental and Analytical Study of Grouted Sleeve Splice Under Axial Tensile Load

**Table AP 2: Summary of parametric study results.**

Name	Bar		Grout	sleeve				Bar Max Force	Bar Max stress	Grout Max Stress	Mode of failure
	$\phi$	Lb	Fg	d out	ts	d in	Ls				
	mm	mm	Mpa	mm	mm	mm	mm				
G200-D12-80-SL48	12	80	50	48.26	7.14	33.98	180	42.3	378.3	21	Bar to Grout Bond Failure
G200-D12-100-SL48	12	100	50	48.26	7.14	33.98	220	47.7	430.82	27.6	Bar to Grout Bond Failure
G200-D12-120-SL48	12	120	50	48.26	7.14	33.98	260	49.2	435.24	21.9	Bar to Grout Bond Failure
G214-D12-80-SL48	12	80	70	48.26	7.14	33.98	180	47.3	418.44	26.5	Bar to Grout Bond Failure
G214-D12-100-SL48	12	100	70	48.26	7.14	33.98	220	51.5	455.59	25.7	Bar to Grout Bond Failure
G214-D12-120-SL48	12	120	70	48.26	7.14	33.98	260	65.6	580.33	55.5	Bar Fracture
G295-D12-80-SL48	12	80	80	48.26	7.14	33.98	180	51.9	459.13	30.12	Bar to Grout Bond Failure
G295-D12-100-SL48	12	100	80	48.26	7.14	33.98	220	57.6	509.55	29.3	Bar to Grout Bond Failure
G295-D12-120-SL48	12	120	80	48.26	7.14	33.98	260	63.6	562.63	34.1	Bar Fracture
G200-D16-100-SL60	16	100	50	60.33	8.74	42.85	220	85.9	427.45	25.6	Bar to Grout Bond Failure
G200-D16-130-SL60	16	130	50	60.33	8.74	42.85	280	100.2	498.61	25.5	Bar to Grout Bond Failure
G200-D16-160-SL60	16	160	50	60.33	8.74	42.85	340	118.8	591.16	26.6	Bar Fracture
G214-D16-100-SL60	16	100	70	60.33	8.74	42.85	220	95.6	475.72	36.2	Bar to Grout Bond Failure
G214-D16-130-SL60	16	130	70	60.33	8.74	42.85	280	108	537.42	37.5	Bar Fracture
G214-D16-160-SL60	16	160	70	60.33	8.74	42.85	340	115	572.25	38.1	Bar Fracture
G295-D16-100-SL60	16	100	80	60.33	8.74	42.85	220	113.9	566.78	43.2	Bar Fracture
G295-D16-130-SL60	16	130	80	60.33	8.74	42.85	280	130.8	650.88	44.16	Bar Fracture
G295-D16-160-SL60	16	160	80	60.33	8.74	42.85	340	141.6	704.62	69.3	Bar Fracture

**Table AP 2: summary of parametric study results.(continued)**

Name	Bar		Grout	sleeve				Bar Max Force	Bar Max stress	Grout Max Stress	Mode of failure
	$\phi$	Lb	Fg	d out	ts	d in	Ls				
	mm	mm	Mpa	mm	mm	mm	mm				
G200-D20-120-SL7 <sub>3</sub>	20	120	50	73.03	7.01	59.01	260	103.8	330.57	95.4	Grout to Sleeve Bond Failure
G200-D20-160-SL7 <sub>3</sub>	20	160	50	73.03	7.01	59.01	340	111.6	355.41	33.2	Bar to Grout Bond Failure
G200-D20-200-SL7 <sub>3</sub>	20	200	50	73.03	7.01	59.01	420	132.9	423.25	110	Grout to Sleeve Bond Failure
G214-D20-12-SL7 <sub>3</sub>	20	120	70	73.03	7.01	59.01	260	110.9	353.18	42.7	Bar to Grout Bond Failure
G214-D20-160-SL7 <sub>3</sub>	20	160	70	73.03	7.01	59.01	340	149.4	475.8	62.2	Bar to Grout Bond Failure
G214-D20-200-SL7 <sub>3</sub>	20	200	70	73.03	7.01	59.01	420	161.3	513.69	61.7	Bar to Grout Bond Failure
G295-D20-120-SL7 <sub>3</sub>	20	120	80	73.03	7.01	59.01	260	133.3	424.52	67.2	Bar to Grout Bond Failure
G295-D20-160-SL7 <sub>3</sub>	20	160	80	73.03	7.01	59.01	340	165.4	526.75	72.8	Bar Fracture
G295-D20-200-SL7 <sub>3</sub>	20	200	80	73.03	7.01	59.01	420	173.9	553.82	60	Bar Fracture
G200-D22-140-SL8 <sub>8</sub>	22	140	50	88.9	7.62	73.66	300	121.6	320.05	35.2	Bar to Grout Bond Failure
G200-D22-180-SL8 <sub>8</sub>	22	180	50	88.9	7.62	73.66	380	195.9	515.61	48.7	Bar to Grout Bond Failure
G200-D22-220-SL8 <sub>8</sub>	22	220	50	88.9	7.62	73.66	460	185.7	488.76	45	Bar to Grout Bond Failure
G214-D22-140-SL8 <sub>8</sub>	22	140	70	88.9	7.62	73.66	300	209.9	552.46	72.2	Bar Fracture
G214-D22-180-SL8 <sub>8</sub>	22	180	70	88.9	7.62	73.66	380	218.7	575.62	66.3	Bar Fracture
G214-D22-220-SL8 <sub>8</sub>	22	220	70	88.9	7.62	73.66	460	227.7	599.31	61.9	Bar Fracture
G295-D22-140-SL8 <sub>8</sub>	22	140	80	88.9	7.62	73.66	300	215.8	567.98	71.8	Bar Fracture
G295-D22-180-SL8 <sub>8</sub>	22	180	80	88.9	7.62	73.66	380	259.7	683.53	72.8	Bar Fracture
G295-D22-220-SL8 <sub>8</sub>	22	220	80	88.9	7.62	73.66	460	300.7	791.44	75.7	Bar Fracture



## Experimental and Analytical Study of Grouted Sleeve Splice Under Axial Tensile Load

**Table AP 3: comparison between the parametric study results and the equation 2 results.**

Name	Bar Max Force from Parametric study	Bond stress from parametric study	bond stress from eq (4.2)	$\eta$ %
	Kn	MPa	MPa	
G295-D20-160-SL73	165.4	16.46	18.11	90.87
G200-D22-180-SL88	195.9	15.75	15.86	99.35
G214-D22-140-SL88	209.9	21.70	20.77	104.49
G214-D22-180-SL88	218.7	17.59	18.76	93.73
G214-D22-220-SL88	227.7	14.98	16.76	89.42
G295-D22-140-SL88	215.8	22.31	22.21	100.48
G295-D22-180-SL88	259.7	20.89	20.06	104.12
G200-D12-100-SL48	47.7	12.66	12.24	103.43
G200-D12-120-SL48	49.2	10.88	11.39	95.52
G214-D12-80-SL48	47.3	15.69	15.49	101.32
G214-D12-100-SL48	51.5	13.67	14.48	94.38
G295-D12-80-SL48	51.9	17.22	16.56	104.00
G295-D12-100-SL48	57.6	15.29	15.48	98.74
G295-D12-120-SL48	63.6	14.07	14.41	97.62
G200-D16-100-SL60	85.9	17.10	16.59	103.06
G200-D16-130-SL60	100.2	15.34	15.32	100.15
G200-D16-160-SL60	118.8	14.78	14.05	105.22
G214-D16-100-SL60	95.6	19.03	19.63	96.93
G214-D16-130-SL60	108	16.54	18.12	91.24
G295-D16-130-SL60	130.8	20.03	19.38	103.36
G295-D16-160-SL60	141.6	17.62	17.77	99.15